Received: 24 September 2021 | Revised: 30 March 2022 | Accepted: 22 April 2022

DOI: 10.1002/tal.1941

RESEARCH ARTICLE

WILEY

Robust structural control of a real high-rise tower equipped with a hybrid mass damper

Lefteris Koutsoloukas[1] | Nikolaos Nikitas[1] | Petros Aristidou[2]

[1]School of Civil Engineering, University of Leeds, Leeds, UK

[2]Department of Electrical Engineering & Computer Engineering and Informatics, Cyprus University of Technology, Limassol, Cyprus

Correspondence
Nikolaos Nikitas, School of Civil Engineering, University of Leeds, LS2 9JT Leeds, UK.
Email: N.Nikitas@leeds.ac.uk

Summary

In this paper, the robust control of a real high-rise tower is studied, using a newly proposed, in the structural control field, Robust Model Predictive Control scheme (RMPC). Two RMPC controllers were designed considering either displacement mitigation ($RMPC_1$) or power consumption efficiency ($RMPC_2$). The two controllers were compared to the benchmark, robustness-wise, H_∞ control scheme to demonstrate their relative performance. A number of stiffness and damping uncertainty scenarios were designed based on a broad study of the relevant literature, in order to estimate the robustness of each of the three controllers. In all scenarios, variable actuator uncertainty of $\pm 5\%$ was introduced. It was found that all controllers are effective in controlling the tower and demonstrate robustness against parametric and actuator uncertainties with different relative merits over each other. Indicatively, when considering root-mean-square (RMS) and peak displacement and acceleration reduction, the H_∞ had an average performance reduction of 24%, the $RMPC_1$ 31% and the $RMPC_2$ 28% against their uncontrolled equivalent.

KEYWORDS

actuator uncertainty, parametric uncertainty, robust controller, Robust Model Predictive Control, structural control, tall Buildings, tuned mass damper

1 | INTRODUCTION

Over the last decades, the structural control sector has gained great attention aiming to propose solutions on suppressing structural vibrations due to wind and earthquake excitations[1–3] or due to human action.[4,5] Applications of passive and active structural control systems are effectively employed on buildings and bridges all around the world.[6–8] When considering the real-life control of civil structures, one expects to face various types of uncertainties within the design process. The introduction of uncertainty within the simulations is of high importance since, in most cases, simulation conditions are considered to be highly idealized, which is far from a realistic scenario where randomness and uncertainty seem to prevail. Forrai et al[9] mentioned that, even extremely detailed models are likely to contain parameter uncertainties and, to deal with this phenomenon, robust control schemes are required. The main types of uncertainty that are considered within the structural control literature are parameter uncertainties that occur due to modeling errors, environmental effects and structural damage, and input uncertainties that occur mainly due to noisy feedback signals and unknown force parameters. In the literature, there are various studies which consider robust algorithms and methodologies, and the performance of passive,[10] semi-active,[11–13] active,[14] and hybrid[15] structural control systems is investigated. In this work, some examples of robust control that can be found in the literature are included and they are organized based on the type of uncertainty

they are considering. Figure 1 summarizes all the studies included within this document to clearly demonstrate the algorithms used for a given type of uncertainty.

This study will investigate the Robust Model Predictive Control (RMPC) and compare it to a well established robust controller benchmark within the structural control field, the H_∞,[1,9,16–21] in order to asses its performance. The RMPC was already implemented in various applications outside the structural control field. For example, Tettamanti et al[22] studied the performance of a RMPC scheme for the control of urban road traffic networks. More specifically, they developed an algorithm with the objective of minimizing the queue lengths within an urban road network under uncertain conditions concluding that the RMPC is an appropriate choice for the specific control application. Mirzaei et al[23] implemented a RMPC for the rotor control of a wind turbine. To demonstrate its effectiveness, the authors compared its performance with a standard Proportional-Integral (PI) controller. Langthaler and del Re[24] developed a RMPC scheme for the control of a diesel engine airpath since in the diesel engine control schemes, it is frequent to come across uncertainties and model-plant mismatch. They showed that their RMPC implementation can be efficient in controlling the diesel engine airpath under the considered uncertainties. Alexis et al[25] implemented a RMPC for the flight control of an unmanned aircraft under uncertain conditions. They demonstrated the performance of their algorithm by experimentally evaluating it in real-time using two unmanned rotorcraft configurations. They concluded that the proposed scheme demonstrated robustness since it effectively dealt with forcible disturbances while having a minimum deviation from the reference trajectory. Maasoumy et al[26] developed a RMPC solution for the robust control of an energy efficient building with box-constrained disturbance uncertainties. The authors compared the RMPC with a nominal MPC and a Rule Based Controller (RBC) to establish their relative performance. They concluded that, when their model uncertainty was between 30% and 67%, the RMPC had the best overall performance, while in the case with lower uncertainty, the nominal MPC was more efficient and in the case with higher uncertainty ($\geq$ 67%), the RBC had the best performance. Nagpal et al[27] developed their RMPC with linear matrix inequalities for the climate control of a building with uncertain model parameters. When comparing the performance of the RMPC to a nominal MPC, which was synthesized without accounting for any model uncertainties, it was found that, the RMPC had a better tracking performance by 24% when considering 70% variation in the system parameters. Additionally, in the presence of severe uncertainty with sinusoidal variations, the RMPC had a 17% better tracking performance than the nominal MPC controller.

In general, various examples of MPC applications can be found in the literature specific to civil engineering control systems, demonstrating the effectiveness of the actual scheme.[28–39] To the authors' best knowledge, the RMPC has not been applied for the vibration mitigation of a real high-rise building application before. For this reason, the effectiveness of the RMPC will be demonstrated within this study, by developing two controllers; one designed for the best possible response mitigation performance, and one designed for reduced power consumption.

In terms of uncertainty, this study will investigate the vibration control of a real tower with parametric and actuator uncertainties. In civil engineering, parametric uncertainties are associated with deviations between the real structure and its mathematical description used for the control design.[6,40] Parameter uncertainties can also occur due to the random and distributed nature of applied loads,[41] due to structural degradation and due to damage.[42] The effect of parameter misalignment between model and real structure may result to poor control design where performance is compromised, and potentially, stability issues may arise.[16] As stated by Lago et al,[43] the damping characteristics of the structural systems are highly uncertain until the building is complete. Moreover, they state that to increase the building's sustainability, it is important to account for the structural model variability.

Uncertainty in the actuator performance may occur in the manufacturing process, which results to individual differences between nominally similar actuators. Moreover, the performance of an actuator can degrade due to long-term use.[44,45] Additionally, it is often that the actuators installed on structures are only periodically inspected/calibrated leading to poor performance.[46] The actuator uncertainty could be associated with instability and poor control performance[44,45] thus, it is crucial to also consider its effect within the simulation process.

This work is structured as follows: Sections 1.1 and 1.2 include an extended review of studies which dealt with parametric and input uncertainty, respectively. Sections 2.1–2.3 include the mathematical derivation of the system dynamics and the detailed description of the novel controller that is used within this study. Section 3 describes the real-life application that is used as a case study. Sections 4 and 5 discuss the results and compare the associated simulations of the simulations while Section 6 concludes the study highlighting the most critical findings.

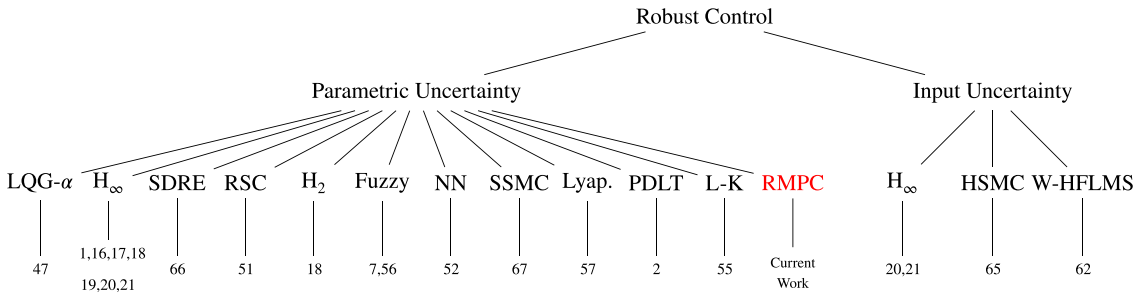

FIGURE 1 Summary of the studies included within this document indicating the gap this study aims to cover

1.1 | Parametric uncertainty

Wang[47] proposed a Linear Quadratic Gaussian- α (LQG- α) algorithm that aimed to provide robust control to earthquake and wind-excited benchmark problems[48,49] while accounting for $\pm 15\%$ stiffness variation with an additional large -25% stiffness perturbation in the wind excitation scenario. They developed the controller so that it provides adjustable relative stability and introduces a gain parameter via a LQG design. The relative stability not only delivers a guaranteed settling time for the system but also increases the controlled system robustness. The author states that in both wind and earthquake loading cases, the proposed algorithm further improves the control performance of the system when compared to a regular LQG. In the case of earthquake, it was mentioned that the LQG- α needed a higher control force than the LQG controller. When the two controllers were saturated to the same control force, it was found that the LQG- α demonstrated robustness also to saturation effects.

Yang et al[1] proposed two H_∞ control strategies for the control of a 76-story benchmark building[49] under wind excitation, and a long-span benchmark bridge[50] subjected to earthquake(s). Their first H_∞ based control strategy was designed to deal with an energy-bounded class of excitations. Their second control strategy was designed for a class of excitations with a specified bounded peak. Both control strategies were compared to a LQG control scheme and simulations were carried out for three different sets of stiffness uncertainty (0%, -15%, and $+15\%$). It was concluded that the newly proposed control schemes outperformed the LQG controller demonstrating in this way their effectiveness.

Stavroulakis et al[18] considered the active control of a two-dimensional 8-story building structure by studying the performance of three algorithms namely, the Linear Quadratic Regulator (LQR), the H_2, and the H_∞. They stated that the LQR and H_2 cannot explicitly account for system uncertainties, and thus, the H_∞ was also considered. The authors introduced parametric uncertainties by using the linear fractional transformation (LFT) method with percentage perturbations. To derive the nominal values for the mass, stiffness, and damping matrices, finite element (FE) models were used. For their control scheme, the authors introduced four actuators co-located with the sensors on the structure. When tested under periodic sinusoidal horizontal loading pressure on each joint, the maximum displacement reduction percentages achieved with the LQR, H_2, and H_∞ were 69.5%, 93.1%, and 86.2%, respectively, always with reference to the uncontrolled case. Their conclusions mention that, even though all the control solutions have proven to be effective, the H_2 and the H_∞ were preferred since they demonstrated enhanced robustness properties.

Lim[51] proposed a robust saturation controller (RSC) that is designed by using Lyapunov robust stability for an uncertain linear time invariant (LTI) system. To improve the control performance, the author proposed a method that considers the optimization of linear matrix inequalities (LMI). The author experimentally tested the proposed controller using a 2-DOF model with parameter (stiffness) uncertainty. The stiffness uncertainty was bounded between $\pm 20\%$. The controller with and without the LMI optimization method was tested and compared against other previously designed controllers (i.e., a LQR controller and a modified bang-bang controller (MBBC)). It was found that the proposed controller method reduced peak drifts of each story by 30.66% and 34.99% for the nominal system against the uncontrolled case. Moreover, it was shown that, as the bounds of the parameter uncertainties were increasing, the MBBC had a better performance than the RSC, while the LQR had the worst performance. When the algorithms were compared in $\pm 20\%$ stiffness uncertainty scenarios, it was concluded that the MBBC could not be used efficiently in an uncertain system even though in most cases it had superior performance over the RSC since, in one of the uncertain scenarios considered, the algorithm lost its robustness due to an unstable mode.

Huo et al[17] investigated a general implementation of the H_∞ controller for an active mass damper (AMD). Their aim was to keep a good vibration dissipation performance while having structural mass and stiffness uncertainties. To model the uncertainties in the system, they used LFT. Moreover, for the design of the H_∞ controller, an efficient solution procedure based on linear matrix inequalities (LMI) was utilized. For their testing model, a two-story flexible structure testbed with an AMD was used and tested under ground accelerations. In their experiment, they introduced a 10% uncertainty in the mass and 40% on the stiffness and damping matrices. For comparison purposes, they designed a pole-placement controller and they showed that, the H_∞ controller had a better performance when having stiffness and mass variation in the model, showcasing in this way the robustness merits. More specifically, four uncertain cases were considered experimentally with different mass uncertainty values and it was shown that, the reduction ratios of the proposed H_∞ controller and the pole-placement controller with respect to the uncontrolled case were $\approx$ 63% and $\approx$ 52% respectively, in the case with no additional mass and, $\approx$ 58% and $\approx$ 20% respectively, with uneven additional mass on both floors.

Narasimhan[52] developed a single hidden layer non-linearly parametrized neural network (NN) with a proportional derivative type controller for the active control of a highway bridge benchmark study[53] with bi-linear isolation devices. The direct Lyapunov approach was used in order to derive adaptive parameter update laws. The proposed control scheme provides robustness since the controller parameters are updated on-line. The author mentioned that the main advantage of the proposed controller is the fact that there is no need for identification before using the controller. Finally, when the controller was used in the control of the highway bridge benchmark, it was concluded that it was efficient in reducing critical responses.

Mohtat et al[7] investigated the trade-off between nominal performance and robustness in both conventional and intelligent[54] structural control schemes. The authors proposed a systematic treatment on stability robustness and performance robustness by taking into account uncertainty that arises from structural parameters. To demonstrate their results, they used a truss bridge under seismic excitation. For the control of

their active tuned mass damper (ATMD), the authors developed a genetic fuzzy logic controller (GFLC), reduced-order observer-based controllers based on pole-placement and LQR schemes. It was found that the fuzzy logic controller was the best choice in terms of compromising between performance and robustness.

Du et al[55] studied the application of Lyapunov–Krasovskii (L–K) approach to develop a sampled data controller for a linearly parameter varying (LPV) model. The controller was investigated on a three-story shear building with an active bracing system. The authors utilized $\pm 40\%$ stiffness and damping uncertainties. It was concluded that the proposed controller is effective on the disturbance attenuation of the model with parameter uncertainty and actuator saturation.

Ding et al[2] proposed a controller based on parameter-dependent Lyapunov theory (PDLT) and the LMI technique for the control of a linear parameter varying model of a three-story building model equipped with an active brace system. The authors utilized mass, stiffness, and damping uncertainty up to $\pm 40\%$. Moreover, the actuator saturation and control forces input time-delay were also taken into account for the control scheme. When the system was tested under seismic excitation, it was found that the proposed controller decreases the building responses, while being simple and practical making it this way a good option for real applications.

Aly[56] first proposed a design approach for a passive tuned mass damper (TMD) to be efficient in parametric uncertainties. Thus, the effectiveness of the optimum parameter passive TMD design was demonstrated, and then the robust parameters of the TMD were presented for a structure with $\pm 10\%$ stiffness uncertainty. The proposed approach was tested on a high-rise building under wind excitation. Due to the slenderness of the building, an actuator was introduced to dissipate the responses in one direction, resulting to an ATMD. Two algorithms were tested for the control of the ATMD namely, LQG and fuzzy logic controller. It was concluded that, regarding the passive TMD with predetermined optimal parameters that take into account structural uncertainties, the system presented robustness. In the case of the ATMD, the fuzzy logic controller demonstrated higher robustness than the LQG. More specifically, when considering the peak displacement reductions, it was shown that the TMD managed to reduce the displacements by 47.45%, 28.50%, and 47.78% for 0%, -10%, and $+10\%$ stiffness uncertainty, respectively. For the same uncertain scenarios the LQG managed to reduce the peak displacements by 52.25%, 45.19%, and 52.60%, whereas the fuzzy logic controller achieved a reduction of 45.80%, 27.60%, and 51.06%, respectively. The fuzzy logic controller managed to reduce (over the LQG controller) the required root-mean-square (RMS) control forces up to 25.66%.

Giron and Kohiyama[57] proposed a robust decentralized control method for the reduction of vibrations on buildings based on the Lyapunov-control function. Moreover, an expression for semi-active control was also proposed by the authors. Using a single-DOF system, the authors demonstrated the effectiveness of the algorithm and its robustness against $\pm 15\%$ stiffness and mass uncertainties.

Huo et al[19] proposed an H_∞ controller for civil engineering structures. For their controller design, the authors used the D-K iteration procedure.[58] To extract the parametric uncertainties from the model matrices, the LFT approach was used. The authors introduced $\pm 10\%$, $\pm 20\%$, and $\pm 30\%$ uncertainty on the mass, damping, and stiffness components. To validate the robustness of their proposed controller, the authors used a 4-DOF mathematical building model and a two-story experimental physical building tested on a seismic table.

Gill et al[59] investigated the robustness of their proposed distributed TMDs and compared their performance to a single TMD and to multiple TMDs installed at the top of a building. For their simulations, they used a 20-story benchmark building[60] subjected to seismic loading. To demonstrate the robustness of their scheme, $\pm 15\%$ stiffness and damping uncertainties were introduced within their simulations. It was found that, the distributed TMDs outperformed the other aforementioned control systems, and their performance in presence of parametric uncertainties was found to be better than the other schemes, especially in the drift and acceleration responses.

Aggumus and Guclu[16] investigated the semi-active control of a 10-story building using a magnetorheological (MR) damper equipped TMD, operating with an H_∞ controller. For their control scheme, they took into account the effects on the system response with uncertainties caused by high frequencies that are not taken into account in their reduced model. The authors studied their control scheme experimentally on a shaking table to assess its performance. It was found that the H_∞ semi-active controlled scheme outperformed the passive TMD in the response reduction of the system. As an example, the best semi-active control scheme had an inter-story drift ratio of 0.236 with respect to the uncontrolled case while the TMD achieved 0.256.

1.2 | Input uncertainty

Wang et al[20,21] developed a robust controller that considers parameter, control effort, and input (disturbance) uncertainties. The authors state that they considered two types of uncertainties, structured, and unstructured[61] for parameter and input, respectively. For the control part, the authors proposed a robust H_2 optimality together with robust H_∞ disturbance attenuation and robust relative stability. It is noted that, the authors considered a singular value decomposition (SVD) for all structured uncertainties. For the demonstration of the performance of the controller, the authors used a 4-DOF mathematical model with $\pm 10\%$ uncertainty in the mass, stiffness, and damping matrices.

Adeli and Kim[62] proposed a wavelet-hybrid feedback-least-mean-square (LMS) algorithm for the robust control of a benchmark study[63] for a 3-DOF system with an AMD and a mass with an ATMD,[64] respectively. It is noted that the original hybrid feedback-least-mean-square algorithm was proposed in their companion paper.[64] The authors mention that, what makes the algorithm robust is the fact that it takes into account

different external disturbances and a large frequency range of vibrations. More specifically, the authors used a low-pass filter that allows all the lower frequency signal components to pass unchanged. The authors add that the high frequency components obstruct the stabilization of filter coefficients (introduced in their companion paper), and thus, by keeping them out, it allows the hybrid feedback-LMS control algorithm to adapt its coefficients in a more stable fashion. In the civil engineering area, this can be effective since, typically the high frequencies of the external excitations do not affect considerably structural response. Based on their results, it was found that, in order to have the best control performance, the cut-off frequency should be 1.5–2 times higher than the largest significant natural frequency. Finally, since the proposed algorithm can be used alongside a feedback controller (i.e., LQR and LQG), it was concluded that the proposed model can be used to enhance the performance of other feedback controllers.

Zhang et al[65] proposed a robust controller which was based on two disturbance observers. More specifically, the authors considered the active control of an offshore wind turbine. For their control scheme, they first initialized two types of disturbances, matched and mismatched for wind and wave loading, respectively. Two non-linear disturbance observers were independently designed to estimate and counteract the unknown disturbances with additional noise. Then a hierarchical sliding mode controller (HSMC) was designed for the control of the wind turbine. It was found that the two disturbance observers had high estimation accuracy and the control algorithm had strong robustness and great vibration mitigation effectiveness.

2 | CONTROL STRATEGY

2.1 | Equations of motion

This section includes the equations of motion of a multi-DOF tower equipped with a mass damper under wind excitation. Equation (1) describes the dynamics of the tower equipped with the mass damper. $M, \hat{C}$, and K denote the mass, structural damping, and stiffness matrices with size $n_{tmd} \times n_{tmd}$, where n_{tmd} represents the dimensionality of the structure with the mass damper. $u_n(t)$ is an m-sized control vector including the actuator uncertainty $(u_n(t) = u(t) + w(t)$, where $u(t)$ is the actuator force and $w(t)$ is the process noise). $\hat{D}$ is a $n_{tmd} \times m$ matrix describing how the control force is entering the system. The external excitations are represented with the r-sized vector $f(t)$ and, matrix E with size $n_{tmd} \times r$ describes the way that the excitations are entering the system. $q(t)$ is the n_{tmd}-sized displacement vector, and the over-dots represent derivatives with respect to time. Lastly, (t) denotes the continuous time variable.[66]

$$M\ddot{q}(t) + \hat{C}\dot{q}(t) + Kq(t) = \hat{D}u_n(t) + Ef(t) \tag{1}$$

Equation (1) can be formulated in an equivalent state-space form with the Equations (2) and (3).

$$\dot{x}(t) = Ax(t) + Bu_n(t) + Hf(t) \tag{2}$$

$$y(t) = Cx(t) + Du_n(t) + v(t) \tag{3}$$

where

$$x(t) = \begin{bmatrix} q(t) \\ \dot{q}(t) \end{bmatrix} A = \begin{bmatrix} 0 & I \\ M^{-1}K & M^{-1}\hat{C} \end{bmatrix}$$

$$B = \begin{bmatrix} 0 \\ M^{-1}\hat{D} \end{bmatrix} H = \begin{bmatrix} 0 \\ M^{-1}E \end{bmatrix} \tag{4}$$

$y(t), C, D$, and v represent the measured outputs, the output matrix, the feedthrough matrix, and the white measurement noise, respectively. Moreover, 0 and I in the matrices in Equation (4) represent the null and identity matrices of appropriate dimensions respectively, and the superscript "-1" represents the inverse matrix operator.

2.2 | Kalman filter

To estimate the states of the system based on measured response data only and to eliminate potential inaccuracies and statistical noise, a discrete Kalman filter is implemented within this work. Using the Equations (2) and (3), the Kalman state estimator is shown in Equation (5).

$$\dot{\hat{x}}(t) = A\hat{x}(t) + Bu(t) + L(y(t) - C\hat{x}(t) - Du(t)) \tag{5}$$

where $\hat{x}(t)$ is the estimated state vector and L is the Kalman gain matrix.[49,50,67,68]

2.3 | Robust model predictive control

The minimax approach for the RMPC design is adopted within this study since it is considered one of the most efficient design techniques.[22] Equations ([6]) and ([7]) show the augmented linear discrete-time prediction model for the RMPC scheme.[24]

$$x(k+1) = A_d\hat{x}(k) + B_d u(k) + Gw_1(k) \tag{6}$$

$$y(k) = C\hat{x}(k) + Du(k) \tag{7}$$

The above system is constrained with $\hat{x}(k) \in \mathbb{X}$ and $u(k) \in \mathbb{U}$ where the sets $\mathbb{X}$ and $\mathbb{U}$ are assumed to be polyhedrons. A_d and B_d are the discrete-time zeroth-order-hold counterparts of matrices A and B[69–71] and $k = \frac{t}{\Delta t}$ is the integer time instant, where Δt is the sampling time.[49] G and $w_1(k)$ represent the actuator uncertainty locator matrix and the uncertainty vector, respectively. $w_1(k)$ is unknown but bounded in some measure, $w_1(k) \in \mathbb{W}_1$, where $\mathbb{W}_1$ is the set of possible uncertainties.

The final optimization problem is highly depended on the set $\mathbb{W}_1$. Lofberg (2003)[72] proposed a box-constrained problem with a single inequality for the set of numbers w_1 such that $\|w_1\|_\infty \le 1$, as seen in Equation (8).

$$\mathbb{W}_1 = \mathbb{W}_\infty = \{w_1 : \|w_1\|_\infty \le 1\} \tag{8}$$

Moreover, Lofberg (2003)[72] proposed a methodology to avoid the intractable problems that occur due to the exponential increase in the computational complexity that will result if the future control effort $u(k+1)$ is to be computed optimally over a control horizon $N_{RMPC} - 1$, using the available $x(k+1)$. Thus, to solve the minimax problem, decision variables $u^{(i)}(\cdot|k)$ and state realization $x^{(i)}(\cdot|k)$ are introduced for every possible uncertainty realization $w_1^{(i)}(\cdot|k)$, where the i superscript denotes the realization index. Finally, the minimax problem is to solve the objective function in Equations (9)–(12). It is noted that the performance measure ℓ is typically assumed to be convex in $x(k+j|k)$ and $u(k+j|k)$ when considering the minimax MPC scheme.[73]

$$\min_{\tau, u^{(i)}(\cdot|k)} \tau \tag{9}$$

subject to

$$\begin{aligned} \ell\Big(\hat{x}^{(i)}(k|k), u^{(i)}(k|k), \ldots, x^{(i)}(k+N_{RMPC}-1|k), \\ u^{(i)}(k+N_{RMPC}-1|k)\Big) \le \tau \end{aligned} \tag{10}$$

$$x^{(i)}(k+j|k) \in \mathbb{X} \tag{11}$$

$$u^{(i)}(k+j|k) \in \mathbb{U} \tag{12}$$

$$\text{for } j = 0, 1, 2, \ldots, N_{RMPC} - 1$$

It is noted that the controllers were designed in Matlab using the YALMIP toolbox[74] and the Gurobi optimizer.[75] This work will not include the full derivation of the H_∞ control scheme for civil engineering structures since, it is extensively used in literature. For the full derivation of the algorithm, the reader can refer to previous works.[16,76,77]

3 | APPLICATION DESCRIPTION

The tower application considered within this study is the 245-m-tall Rottweil tower located in Germany, which is a test tower for high-speed elevators. The tower was designed to satisfy specific requirements when experiencing wind-induced vibrations. Based on observations, the speed of

the wind excitation can reach 15.3–16.7 m/s, referring to ground values at a height of 10m. The wind induced vibrations are primarily of vortex shedding nature and they are expected to cause human discomfort and impact the structural integrity of the tower, especially in terms of long-term fatigue.[78]

To guarantee human comfort while ensuring structural integrity, a uni-directional hybrid mass damper (HMD) was installed which is not an unusual case in buildings, see previous works.[79–81] The term hybrid, arises from the fact that the system combines a passive mass damper, two actuators, orthogonal along the principle axes, with a maximum capacity of 35 kN, and semi-active capabilities with adjustable damping and stiffness parameters. In this paper, only the passive and active components of the control system will be considered, and thus, the system will operate either as a TMD and/or as an ATMD. It is noted that, in the ATMD configuration, the actuators will be adding forces on top of the passive one generated by the naturally moving mass. The installed actuators' capacity is considered to be relatively small when compared to other actuators that are applied on similar sized structures. For reference, the control system equipping the Nanjing TV tower has an actuator capacity of 100 kN[79] and the Shanghai World Financial Center Tower 142.5 kN.[80] The mass of the system was chosen to be 240 t based on closed form formulas,[82] which corresponds to a mass ratio of 1.3%. The tower is equipped with four uni-axial MEMS accelerometers which capture the horizontal accelerations of the tower and the mass damper. Additionally, the displacement of the actuators is monitored using string pot transducers and an inductive length measuring system integrated within the linear motors.[83]

For the simulations of this paper, the authors derived a reduced-order model with 15-DOF. It is mentioned that in this study, the two planes of the building are considered decoupled (i.e., no aeroelastic coupling contribution) and thus, only one plane is considered, which further discards all torsional vibrations. The originally bi-directional HMD is herein used as a uni-directional control system, without though any loss of generality. For the derivation of the reduced-ordered model, the authors followed the same procedure described in Koutsoloukas et al,[31] where a nominal MPC was designed for the control of the same tower and its performance was compared against an LQR and the equivalent passive TMD. The damping matrix was determined using the Rayleigh approximation with critical damping ratio of 1% for modes 1 (0.17 Hz) and 5 (5.88 Hz). All dynamic characteristics are from an updated FE model, while in what is shown later displacements are considered to be the dynamic part-only of the total displacement; the latter incorporating also the static wind component.[84]

4 | NUMERICAL SIMULATIONS OF THE TOWER AND RESULTS

This section includes the results of three simulation scenarios with actuator, stiffness and damping uncertainties. In all scenarios, the peak and RMS responses of the tower on the first, top, and two intermediate floors are presented. Moreover, as it was mentioned in Section 3, the Rottweil tower is used to test high-speed elevators. In order for the elevators to operate properly, the top floor dynamic displacement cannot exceed a manufacturer's tolerance of 200 mm. Thus, a top floor dynamic displacement limit of 200 mm is introduced within this study.

The selected RMPC objective function for the control of the Rottweil tower can be seen in Equation (13) subjected to the constraints in Equations (14)–(16).

$$\min_{u} \max_{w_1} \sum_{j=0}^{N_{RMPC}-1} \|Q_{RMPC}\hat{x}(k)\|_{\infty} + \|R_{RMPC}u(k)\|_{\infty} + aS \tag{13}$$

subject to

$$w_1(k+j|k) \in \mathbb{W}_1 \tag{14}$$

$$u_{min} \le u(k) \le u_{max} \tag{15}$$

$$q_{min} - S \le q(k) \le q_{max} + S \tag{16}$$

Q_{RMPC} and R_{RMPC} are weighting matrices of appropriate dimensions. S is a slack variable used to minimize the soft constraint violation with a being a very large scalar weight. The full algorithm derivation on how the above optimization problem is solved can be found in Lofberg (2003a).[73] The robust optimization is carried out by developing the so-called "robust counterpart" of the uncertain system. The robust counterpart is derived by removing the uncertainty within the system. The full method on developing the robust counterpart of the proposed system can be found in Lofberg (2012).[85]

By using two different combinations of Q_{RMPC} and R_{RMPC}, two different RMPC controllers are developed. $RMPC_1$ is designed to account for the best displacement response dissipation while $RMPC_2$ is designed for a reduced power consumption (P_{act})[49] by penalizing the control effort ($u(k)$) and the actuator velocity ($\dot{q}_{act}(k)$) in the total integration time (Ts) where

$$P_{act}(k) = \dot{q}_{act}(k)u(k) \tag{17}$$

$$RMS(P_{act}) = \left\{ \frac{1}{\frac{Ts}{\Delta t}+1} \sum_{k=0}^{\frac{Ts}{\Delta t}} [P_{act}(k)]^2 \right\}^{1/2} \tag{18}$$

In the RMPC scheme, hard and soft constraints were introduced within the algorithms, as seen in Equations (15) and (16), respectively. To force the algorithm keep the top floor displacement ($q_{15}(k)$) within the desired limit, the q_{min} and q_{max} were set to -200 and 200 mm respectively, and the control input limits u_{min} and u_{max} were set to -35 and 35 kN, respectively. Moreover, due to the tower's architecture, only the top story is usable by humans. Since the floor accelerations are directly related to human comfort,[86] the top floor accelerations are considered of relatively more significance within this study. A schematic diagram is included in Figure 2 showcasing the wind loading on the first, an intermediate (7th), and the top (15th) floor. For the simulations of this paper, all the parametric uncertainties were introduced directly within the stiffness and damping matrices. As mentioned in Section 1, in all scenarios, a random actuator uncertainty within $\pm 5\%$ was considered. This means that, for every control signal calculated by the controller, the final actuator force was randomly selected ranging between 95%–105% of it. All simulations within this study were carried out in Matlab.

4.1 | Scenario 1

As it can be seen in Tables 1 and 2, the TMD and the three controllers had good performance on dissipating the RMS and peak responses of the tower compared to the uncontrolled case. As seen in Table 1, in the uncontrolled case and in the case with the TMD, the top floor displacement exceeded the 200 mm limit that was initially set. This is actually the very reason the Rottweil tower needs incorporating a more effective vibration mitigation solution than the TMD. When considering the controllers, the H_∞ could not decrease the top floor displacement within the desired

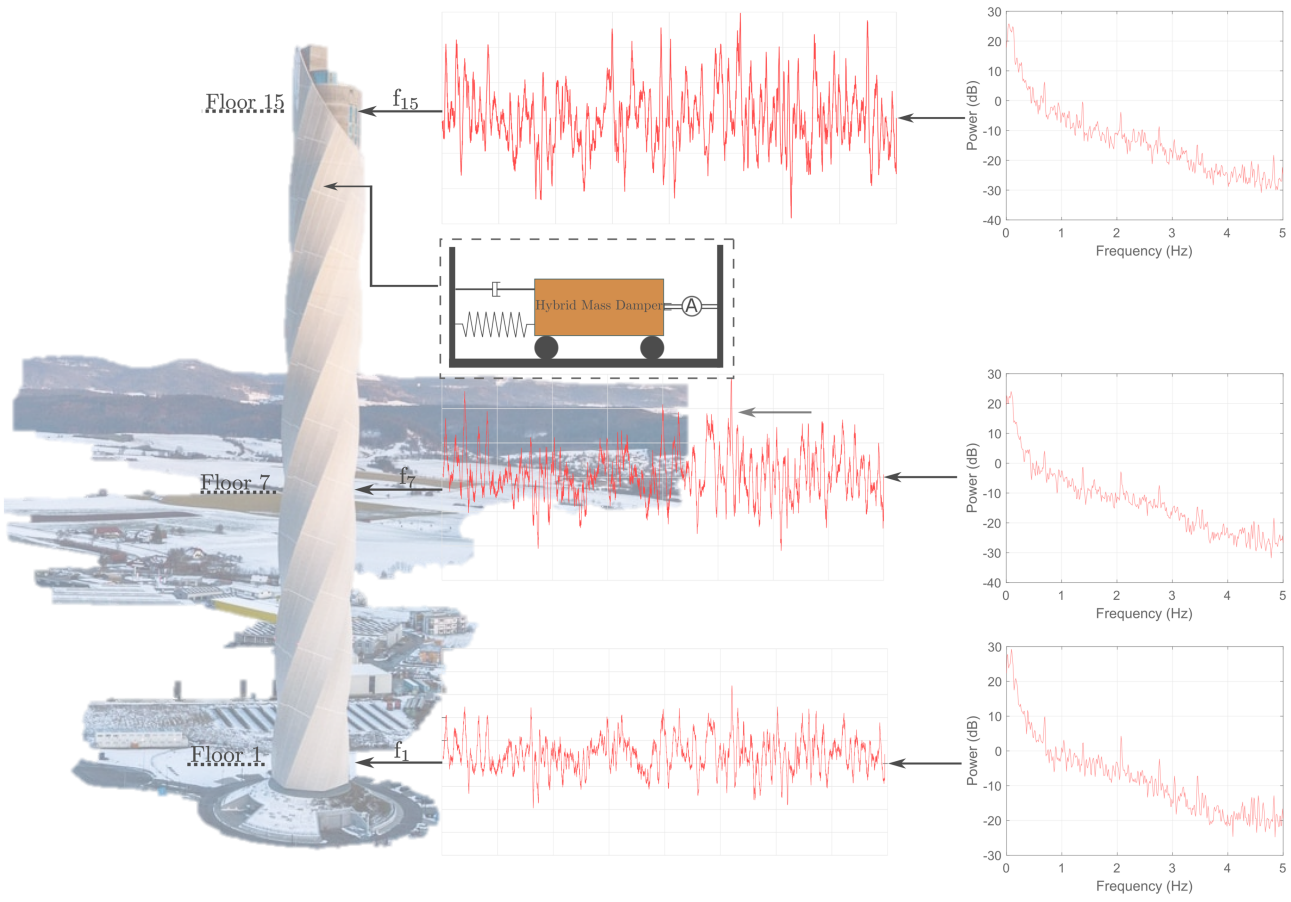

FIGURE 2 Schematic diagram of the wind loading applied on the first, intermediate (7), and top (15) floors

TABLE 1 Maximum and RMS displacement values for the nominal system (0% parameter uncertainty) with ± 5% actuator uncertainty

	RMS					MAX				
Floor No.	Uncontrolled	TMD	H∞	$RMPC_1$	$RMPC_2$	Uncontrolled	TMD	H∞	$RMPC_1$	$RMPC_2$
1	0.05	0.039	0.037	0.035	0.037	0.18	0.16	0.15	0.13	0.14
5	1.43	1.13	1.09	1.03	1.08	5.32	4.83	4.39	3.96	4.12
10	4.31	3.39	3.27	3.10	3.26	16.1	14.6	13.3	11.9	12.4
15	6.65	5.24	5.04	4.79	5.03	24.8	22.6	20.5	18.5	19.0

Note: All units in centimeters.

TABLE 2 Maximum and RMS acceleration values for the nominal system (0% parameter uncertainty) with ± 5% actuator uncertainty

	RMS					MAX				
Floor No.	Uncontrolled	TMD	H∞	$RMPC_1$	$RMPC_2$	Uncontrolled	TMD	H∞	$RMPC_1$	$RMPC_2$
15	6.54	4.10	3.84	3.28	3.92	20.3	17.1	15.5	14.5	12.7

Note: All units in cm/s^2.

limits, even if marginally away from it, while the two RMPC controllers did manage to decrease the top floor displacement below 200 mm. More specifically, the $RMPC_1$ had the best overall response control performance when considering the RMS and peak displacements. Figure 3 shows the top floor displacements of the TMD, H_∞, $RMPC_1$, and $RMPC_2$, respectively, against the uncontrolled case. As seen therein, all the control schemes demonstrated response reduction when compared to the uncontrolled case. The effectiveness of the control systems is also showcased in the auto power spectral densities where the frequency peak at 0.17 Hz in the uncontrolled case is considerably suppressed in all cases. When considering the top floor accelerations, the $RMPC_1$ had the best performance on decreasing the RMS top floor accelerations, while the $RMPC_2$ had the best performance on decreasing the maximum absolute acceleration value; note that acceleration was not included explicitly within the controller objective function. Figure 4 shows the top floor acceleration responses of the TMD and the three controllers compared to the uncontrolled case, and the corresponding power spectra for each case. It is noticed that in the RMPC schemes, there was an observable increase in the acceleration power spectrum in the higher order modes, something quite different to how a TMD would perform. When considering the power consumption of the controllers, the $RMPC_2$ had the lowest RMS value with 2.36 kW and a peak value of 19.9 kW. The H_∞ RMS and peak power consumption were, 3.65 and 16.5 kW, respectively, where the equivalent $RMPC_1$ values were 6.60 and 30.7 kW, respectively. It can be noticed that in order for the $RMPC_2$ to keep the top floor displacement limit of 200 mm and satisfy the soft constraint that was initially set, it required a higher power consumption than the H_∞ scheme. The power consumption of the three controllers against time and the actuator energy consumption in absolute values are presented in Figure 5. It is noted that the energy consumption was calculated as the integral of the absolute of power over time, and thus, it does not alone distinguish between adding or extracting energy from the structure, while it does not also account for additional hardware energy loses (e.g., see actuator efficiency rating). The total actuator energy consumption using the H_∞ controller was 1.05×10^4 kJ from which, the actuators required 4.4×10^3 kJ to remove energy and 6.1×10^3 kJ to add energy to the mass damper motion. When using the $RMPC_1$, the total actuator energy consumption was 1.91×10^4 kJ, where the actuators required 7.7×10^3 kJ to remove energy from the mass damper and 1.14×10^4 kJ to add energy to it. Lastly, the total actuator energy consumption using the $RMPC_2$ was 4.52×10^3 kJ from which the actuators required 2.3×10^3 kJ to remove energy and 2.2×10^3 kJ to add energy to the moving structure. This balance of energy that is spent toward dissipating the mass damper is quite an interesting feature for the purpose of this particular hardware setup. Potentially, it could be handled by a semi-active device on much lower energy expenditure.

4.2 | Scenario 2

Scenario 2 was developed in order to investigate the performance and robustness of the two controllers and the passive TMD in the presence of minor modeling errors and errors possibly relating to light environmental effects as quoted before. As seen in Tables 3–6, the three controllers, H_∞, $RMPC_1$, and $RMPC_2$ demonstrate robustness and are effective in controlling the RMS and peak displacements and accelerations of the tower. However, in all cases, again the H_∞ could not keep the top floor displacements within the desired limit, in contrast to the two RMPC controllers. It is noted that, when the parameter uncertainty was set to −2%, the peak acceleration recorded in the case with the passive TMD was higher even than the one recorded in the uncontrolled case despite the fact that the RMS acceleration was still decreased. One could expect these phenomena since, as it was shown in Rana and Soong (1998),[87] the detuning of a TMD could worsen structural responses. Moreover, as mentioned

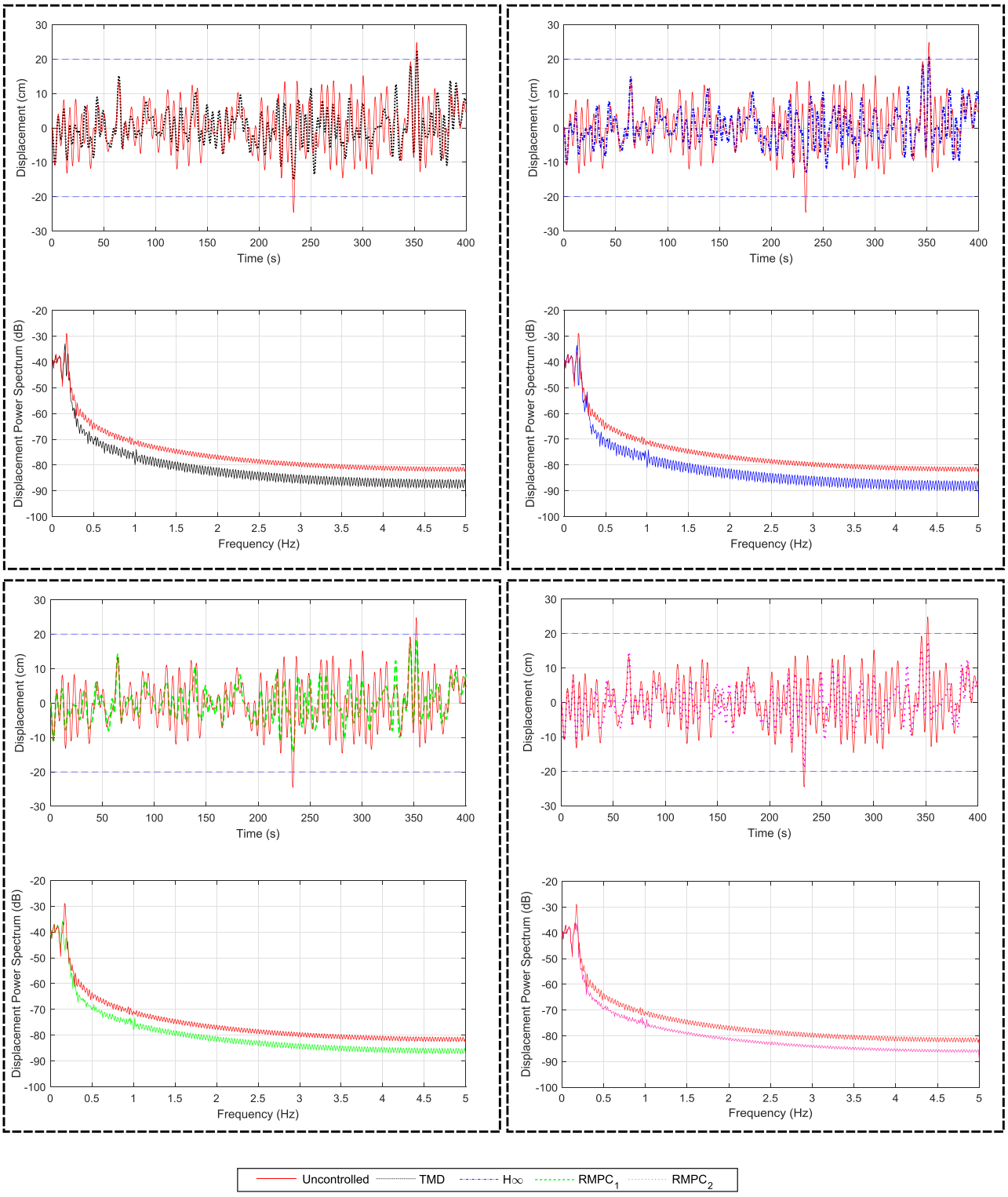

FIGURE 3 Time and frequency analysis of the displacement responses in the controlled and uncontrolled cases

in previous works,[13,88] even small deviations of the primary structure may lead to considerable decrease in performance of passive TMDs. Namely, as filed in Table 6, the maximum acceleration recorded in the uncontrolled case was 17.0 cm/s^2, where in the case with the TMD, the maximum acceleration was 17.5 cm/s^2 which corresponds to 4.6% increase. However, the RMS acceleration was considerably decreased from 6.37 cm/s^2 in the uncontrolled case to a 4.17 cm/s^2 with the TMD, which corresponds to a 34.5% decrease. When considering the controllers, the RMPC$_1$ had the best performance on decreasing the RMS and peak accelerations in both uncertainty cases. When investigating the power

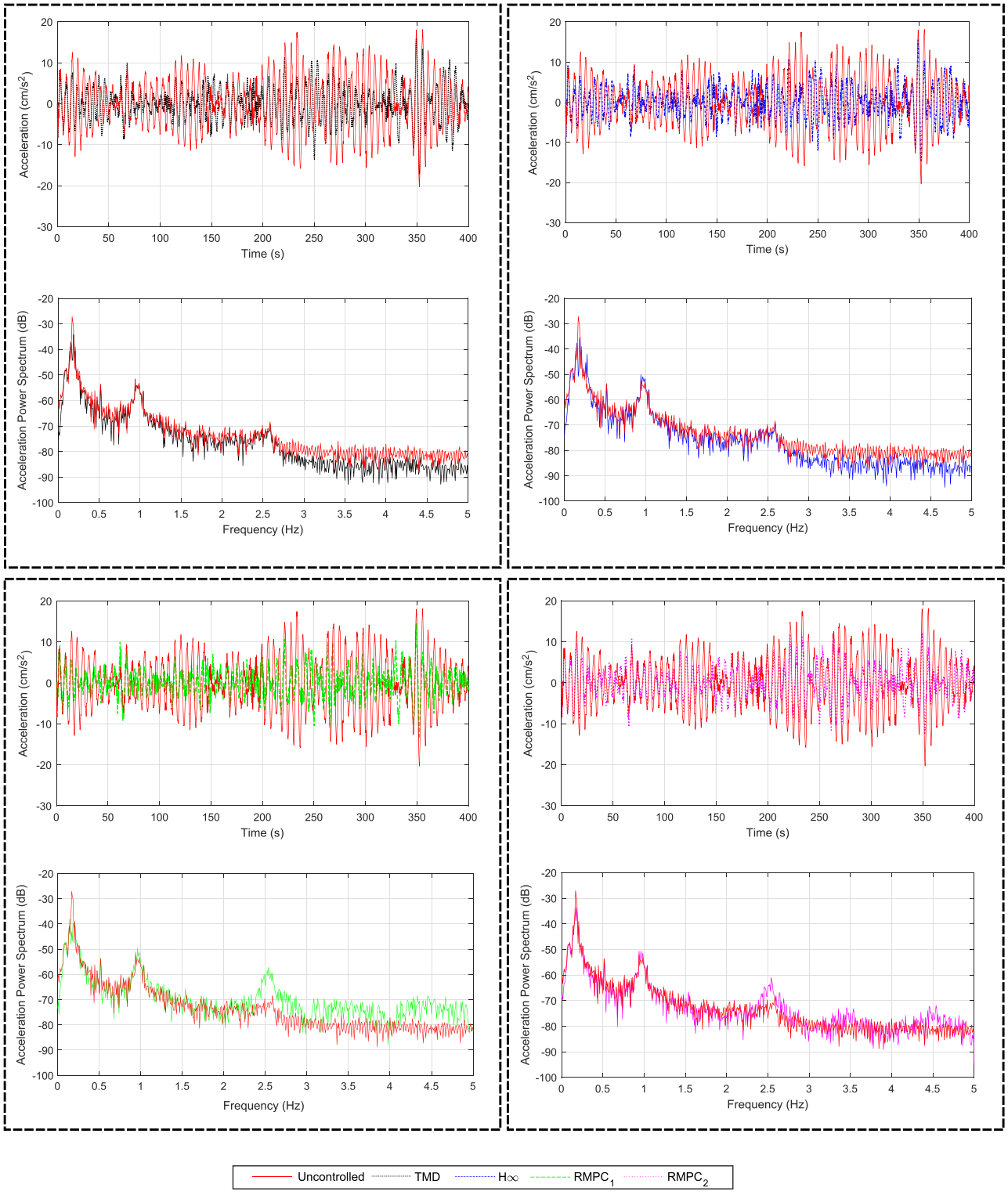

FIGURE 4 Time and frequency analysis of the acceleration responses in the controlled and uncontrolled cases

consumption of the three controllers in the case where the uncertainty was set to +2%, the $RMPC_2$ had the lowest RMS and peak power consumption with 2.13 and 15.8 kW, respectively, were the H_∞ achieved 5.04 and 18.1 kW, respectively, and the $RMPC_1$ 6.42 and 26.0 kW, respectively. In the case where the uncertainty was −2%, the average power consumption for the $RMPC_2$, H_∞, and $RMPC_1$ were 2.28, 5.03, and 7.19 kW, respectively, while the peak power consumptions for the three controllers were 22.3, 17.7, and 32.1 kW, respectively. The total energy requirements for the $RMPC_1$ in the case with +2% was 1.8×10^4 kJ, from which 7.5×10^3 kJ were required for the control system to remove

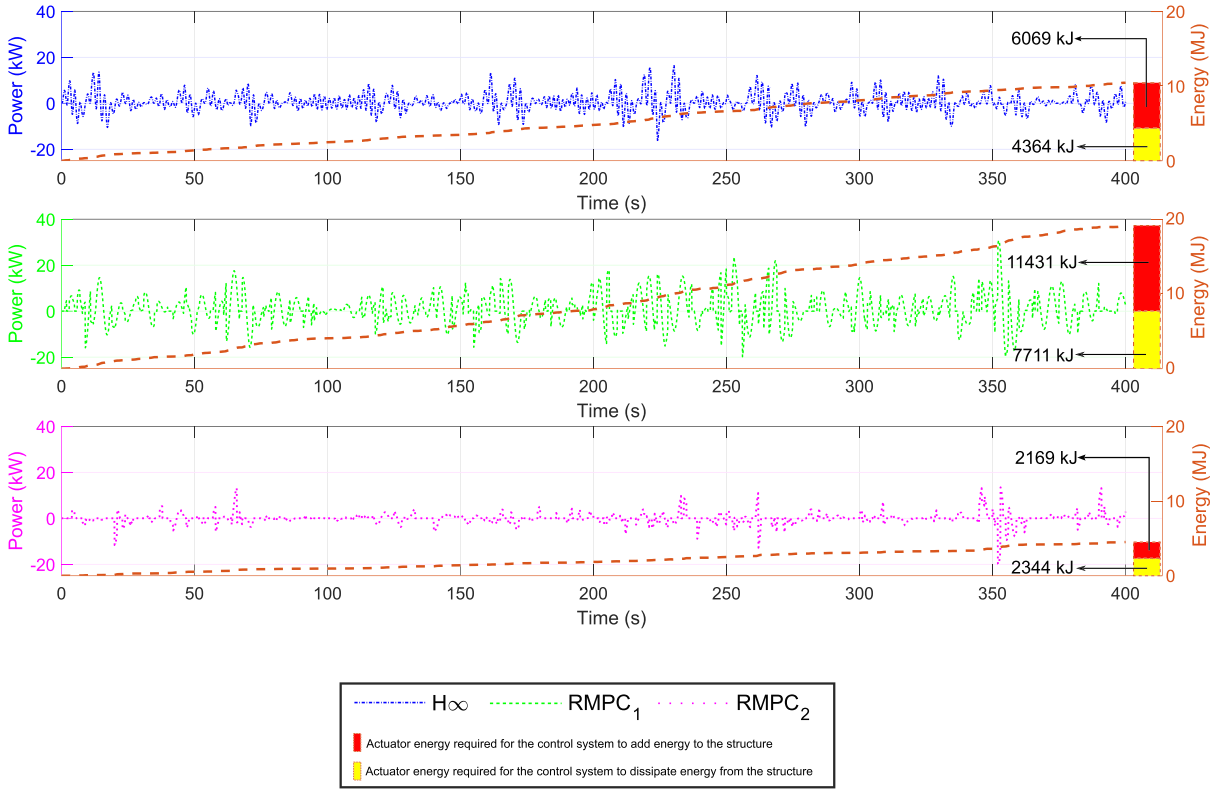

FIGURE 5 Power and energy consumption over time for the active control schemes for the nominal system

TABLE 3 Maximum and RMS values for the system with +2% damping and stiffness uncertainty and ± 5% actuator uncertainty

	RMS					MAX				
Floor No.	Uncontrolled	TMD	H∞	$RMPC_1$	$RMPC_2$	Uncontrolled	TMD	H∞	$RMPC_1$	$RMPC_2$
1	0.049	0.037	0.036	0.034	0.038	0.19	0.15	0.14	0.13	0.14
5	1.45	1.09	1.08	1.01	1.13	5.53	4.67	4.51	4.00	4.21
10	4.38	3.28	3.25	3.02	3.41	16.6	14.14	13.6	12.1	12.7
15	6.76	5.06	5.01	4.67	5.26	25.6	21.8	21.0	18.7	19.6

Note: All units in centimeters.

TABLE 4 Maximum and RMS acceleration values for the system with +2% damping and stiffness uncertainty and ± 5% actuator uncertainty

	RMS					MAX				
Floor No.	Uncontrolled	TMD	H∞	$RMPC_1$	$RMPC_2$	Uncontrolled	TMD	H∞	$RMPC_1$	$RMPC_2$
15	6.91	4.03	3.85	3.30	3.98	19.8	16.7	15.5	14.4	15.2

Note: All units in cm/s^2.

energy from the damper mass and 1.1×10^4 kJ were required to add energy to it. The H_∞ required a total of 1.4×10^4 kJ from which 6.6×10^3 kJ were used to remove energy from the mass damper and 7.3×10^3 kJ were used to add energy to it. Finally, when using the $RMPC_2$, the total energy requirements were 4.3×10^3 kJ from which 2.1×10^3 kJ were used to remove energy from the mass damper and 2.2×10^3 kJ were used to add energy to it. In the case were the uncertainty was set to −2%, the total requirements for the $RMPC_1$, H_∞, and $RMPC_2$ were 2.1×10^4 kJ, 1.5×10^4 and 4.1×10^3 kJ, respectively. The energy required for the three controllers to act as effective break was 8.2×10^3, 7.1×10^3, and 2.1×10^3 kJ, respectively, where the energy required for the control system to act as actuation to the structure was 1.3×10^4, 7.9×10^3, and 2.0×10^3 kJ, respectively.

TABLE 5 Maximum and RMS values for the system with −2% damping and stiffness uncertainty and ± 5% actuator uncertainty

	RMS					MAX				
Floor No.	Uncontrolled	TMD	H∞	$RMPC_1$	$RMPC_2$	Uncontrolled	TMD	H∞	$RMPC_1$	$RMPC_2$
1	0.048	0.039	0.039	0.036	0.040	0.18	0.17	0.16	0.14	0.14
5	1.43	1.17	1.15	1.05	1.18	5.29	5.01	4.85	3.9	4.08
10	4.32	3.52	3.48	3.17	3.56	15.86	15.1	14.6	11.7	12.3
15	6.67	5.44	5.37	4.906	5.50	24.4	23.4	22.7	18.1	19.1

Note: All units in centimeters.

TABLE 6 Maximum and RMS acceleration values for the system with −2% damping and stiffness uncertainty and ± 5% actuator uncertainty

	RMS					MAX				
Floor No.	Uncontrolled	TMD	H∞	$RMPC_1$	$RMPC_2$	Uncontrolled	TMD	H∞	$RMPC_1$	$RMPC_2$
15	6.36	4.17	4.04	3.30	3.89	17.0	17.5	16.3	13.2	13.4

Note: All units in cm/s^2.

TABLE 7 Maximum and RMS values for the system with +10% damping and stiffness uncertainty and ± 5% actuator uncertainty

	RMS					MAX				
Floor No.	Uncontrolled	TMD	H∞	$RMPC_1$	$RMPC_2$	Uncontrolled	TMD	H∞	$RMPC_1$	$RMPC_2$
1	0.046	0.034	0.032	0.031	0.035	0.14	0.14	0.13	0.12	0.12
5	1.38	0.98	0.96	0.90	1.01	4.19	4.16	3.92	3.43	3.55
10	4.17	2.95	2.87	2.69	3.11	12.5	12.6	11.8	10.2	10.7
15	6.43	4.55	4.44	4.15	4.80	19.2	19.5	18.3	15.7	16.5

Note: All units in centimeters.

TABLE 8 Maximum and RMS acceleration values for the system with +10% damping and stiffness uncertainty and ± 5% actuator uncertainty

	RMS					MAX				
Floor No.	Uncontrolled	TMD	H∞	$RMPC_1$	$RMPC_2$	Uncontrolled	TMD	H∞	$RMPC_1$	$RMPC_2$
15	7.15	3.95	3.60	3.12	4.00	18.8	16.3	14.6	15.3	13.3

Note: All units in cm/s^2.

4.3 | Scenario 3

Scenario 3 models the uncertainty that could, as quoted, occur due to major modeling errors and possibly more severe cumulative degradation and damage phenomena. Tables 7–10 collect as above all dynamic response outputs. In Table 9, even for the case of −10% uncertainty, the RMPC1 and RMPC2 showed relatively good performance on decreasing the top floor displacement, yet the 200 mm limit was not satisfied. This demonstrates that the low actuator capacity impels the controller to violate the soft constrain that was initially set as a key requirement of the simulation. In MPC schemes, hard constraints are typically used in control input since it is directly related to physical limitations. For the states, soft constraints are used instead since, in most of the times they cannot be enforced due to the disturbances that are acting on the system.[89,90] Additionally, adding a hard constraint on states may result to an infeasible optimization problem.[91] Moreover, it is noted that in the case where the damping and stiffness uncertainties are set to +10%, the top floor displacement in the case with the passive TMD was slightly increased compared to the uncontrolled scenario. More specifically, and almost counter-intuitively, as seen in Table 7, the maximum displacement recorded at the top floor with the TMD was 19.5 cm where, in the uncontrolled case it was 19.1 cm, demonstrating again a detuning effect. However, even though there was a slight increase in the peak values (2.05%), the TMD managed to decrease the corresponding RMS value by 29.2%. When

TABLE 9 Maximum and RMS values for the system with −10% damping and stiffness uncertainty and ± 5% actuator uncertainty

	RMS					MAX				
Floor No.	Uncontrolled	TMD	H∞	$RMPC_1$	$RMPC_2$	Uncontrolled	TMD	H∞	$RMPC_1$	$RMPC_2$
1	0.051	0.047	0.045	0.041	0.042	0.19	0.19	0.18	0.16	0.16
5	1.5	1.41	1.35	1.20	1.24	5.88	5.68	5.52	4.70	4.91
10	4.52	4.24	4.08	3.61	3.75	17.8	17.2	16.7	14.2	14.8
15	6.99	6.56	6.31	5.57	5.78	27.4	26.5	25.8	21.9	22.8

Note: All units in centimeters.

TABLE 10 Maximum and RMS acceleration values for the system with −10% damping and stiffness uncertainty and ± 5% actuator uncertainty

	RMS					MAX				
Floor No.	Uncontrolled	TMD	H∞	$RMPC_1$	$RMPC_2$	Uncontrolled	TMD	H∞	$RMPC_1$	$RMPC_2$
15	5.88	4.82	4.57	3.96	4.64	20.2	18.3	16.5	15.1	16.9

Note: All units in cm/s^2.

considering the performance of the three controllers, the $RMPC_1$ had again the best performance on decreasing the RMS and peak displacement values of the tower in all the uncertainty cases. Moreover, the $RMPC_1$ was the most efficient in decreasing the RMS and peak accelerations in the case where the uncertainty was set to −10% (Table 10). In the case where the uncertainty was set to +10%, the $RMPC_1$ had the best performance on decreasing the RMS accelerations and the $RMPC_2$ was the most efficient in limiting the peak accelerations (Table 8). Finally, the RMS power consumption of the $RMPC_2$, H_∞, and $RMPC_1$ for the case where the uncertainty was set to +10% was 1.87, 4.66, and 6.46 kW, respectively where the corresponding peak values were 11.2, 17.7, and 30.5 kW, respectively. In the case were the uncertainty was set to −10%, the RMS power with the $RMPC_2$ controller was 2.79 kW, with the H_∞ was 5.77 kW, and with the $RMPC_1$ was 7.52 kW. The corresponding peak power values were 18.8, 19.6, and 30.2 kW, respectively. The total energy requirements for the $RMPC_1$, H∞, and $RMPC_2$ controllers in the case where the uncertainty was set to +10% were 1.8×10^4, 1.3×10^4, and 3.8×10^3 kJ, respectively, while in the case where the uncertainty was set to −10%, the total energy requirements were, 2.2×10^4, 1.7×10^4, and 5.2×10^3 kJ. In the case with +10% uncertainty, the energy required for the control system to remove energy from the mass damper using the three controllers was 7.8×10^3, 6.0×10^3, and 2.0×10^3 kJ where in the case with −10% uncertainty, it was 8.5×10^3, 8.1×10^3, and 2.3×10^3 kJ, respectively. The energy required for the control system to add energy to the mass damper using the three controllers in the +10% uncertainty case was 1.1×10^4, 6.7×10^3, and 1.8×10^3 kJ, respectively, where in the case were the parameter uncertainty was set to −10%, the energy required for the control system to literally actuate the structure using the three controllers was 1.3×10^4, 8.8×10^3, and 2.8×10^3 kJ, respectively.

5 | SUMMARY

Figures 6 and 7 show a summary of the peak and RMS responses, respectively, in different uncertainty realizations for the uncontrolled case, the TMD, the H_∞, the $RMPC_1$, and the $RMPC_2$ schemes. Moreover, Figure 8 shows the maximum and RMS power consumption of the H_∞, the $RMPC_1$, and the $RMPC_2$ control schemes along with the energy requirements of each controller. To further compare more holistically the performance of the three controllers and the TMD, a performance index, $J_{control}$, is introduced (Equation (19)), which considers the control efficacy of each controller in all five uncertain cases (p), against the baseline of the uncontrolled case, where $q_{(i)}$ and $q_{u(i)}$ represent the displacement of the controlled and uncontrolled cases in the corresponding floor (i), and similarly $\ddot{q}_{(15)}$ and $\ddot{q}_{u(15)}$ are the top floor acceleration in the controlled and uncontrolled cases, respectively. It is noted that the smaller the performance index, the better the performance of the control system is.

$$J_{control} = \frac{1}{5}\sum_{p=1}^{5}\left(\frac{1}{4}\sum_i q_{(i)}/q_{u(i)} + \frac{1}{4}\sum_i \mathrm{RMS}(q_{(i)})/\mathrm{RMS}(q_{u(i)}) + \ddot{q}_{(15)}/\ddot{q}_{u(15)} + \mathrm{RMS}(\ddot{q}_{(15)})/\mathrm{RMS}(\ddot{q}_{u(15)})\right)_{(p)} \quad (19)$$

$$\text{for } i = 1, 5, 10, 15$$

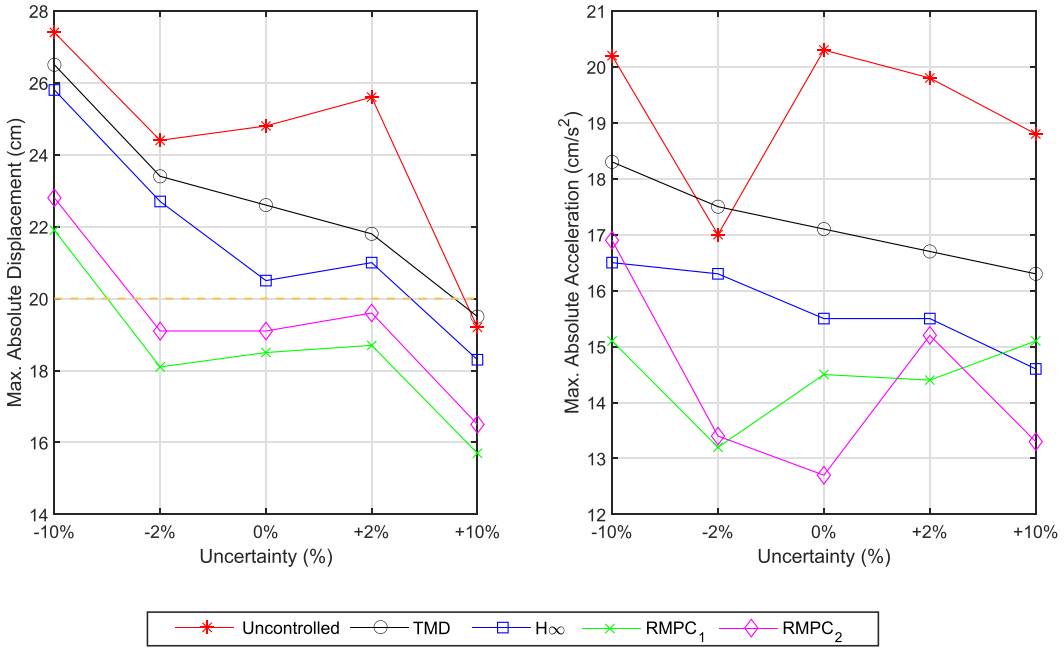

FIGURE 6 Summary of the maximum top floor responses

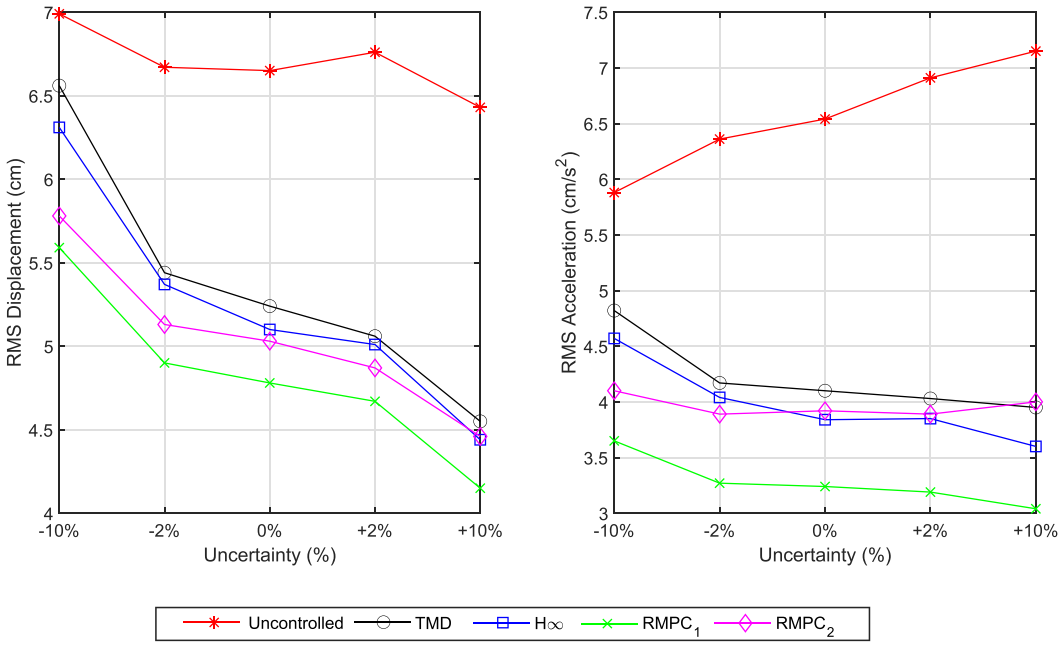

FIGURE 7 Summary of the root-mean-square (RMS) top floor responses

As seen in Figure 9, the $RMPC_1$ had the best overall control dynamic output performance with a performance index $J_{control} = 0.69$ while having the highest power consumption. The H_∞ had a performance index and $J_{control} = 0.76$ while the $RMPC_2$ had a performance index almost right in the middle at $J_{control} = 0.72$. The $RMPC_2$ had the lowest RMS power consumption in all cases and the lowest peak consumption in the −10%, +2%, and +10% uncertainty cases. It is noted that in the remaining cases, the controller sacrificed the power consumption in order to satisfy the soft constrain set for the top floor displacements. As expected, the passive TMD had the worst performance of all control devices with a performance index $J_{control} = 0.80$. This roughly indicates that the distance from the TMD to H_∞ is rather impressively equal to the one from the H_∞ to the less aggressive from the RMPC options.

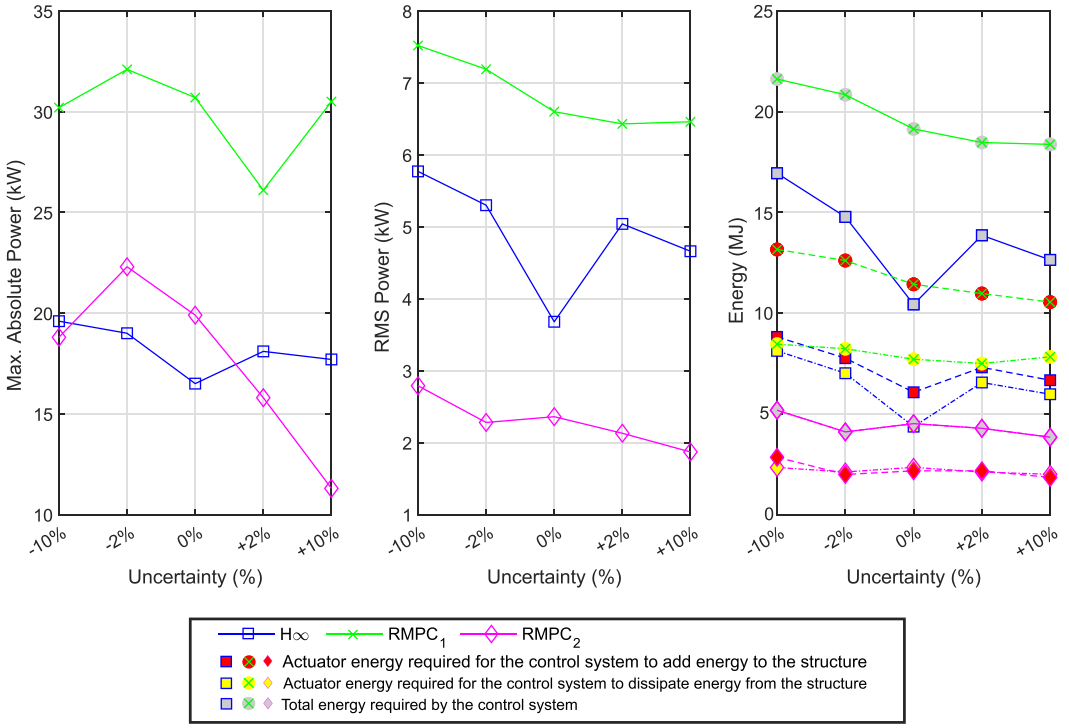

FIGURE 8 Summary of the maximum and root-mean-square (RMS) power, and the energy consumption for each controller

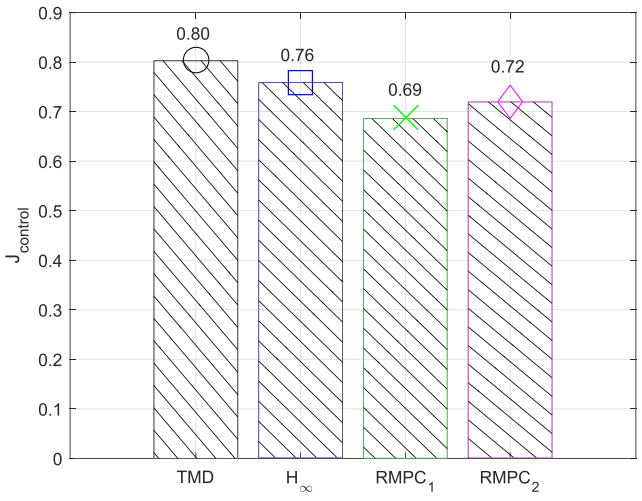

FIGURE 9 Performance index for the control schemes

6 | CONCLUSION

This study considered the robust control of the 245-m tall Rottweil tower using a 2D reduced-order model. Two Robust Model Predictive controllers were developed and compared against the well-established H_∞ control scheme that is widely considered of benchmark value. A so-called $RMPC_1$ controller was designed to account for the best possible displacement control of the tower, while a so-called $RMPC_2$ was designed for reduced power consumption. To account for parameter uncertainties, three different control scenarios were constructed aligning with similar literature studies. In all scenarios, the nominal design wind load (i.e., the only force consideration) was kept the same and no aeroelastic and other intricate response amplitude effects were considered explicitly within the simulations. In all cases, the energy expenditure of the controllers was assessed in detail, separating instances of adding to extracting energy to the mass damper.

Scenario 1 considered the nominal reduced-order model of the tower (0% uncertainty). In Scenario 2, $\pm 2\%$ damping and stiffness uncertainties were introduced to simulate minor modeling errors, presumably owing to light environmental effects or even human occupancy. Lastly, Scenario 3 simulated more considerable modeling errors such as those linked to cumulative aging, and structural damage and thus, it considered $\pm 10\%$ damping (a value within, or even lower than, the accuracy of tracking damping) and stiffness uncertainties. Moreover, in all scenarios a variable actuator uncertainty randomly ranging between $\pm 5\%$ was introduced, which is the maximum expected uncertainty of the installed actuators. It was found that all three controllers demonstrated robustness and effectiveness on dissipating the displacement and acceleration responses of the actual tower in all parametric scenarios. As probably expected, the passive TMD did not demonstrate consistent robustness since, in Scenario 2 with -2% damping and stiffness uncertainty, the top floor accelerations were more severe when compared to the uncontrolled case, and in Scenario 3 with $+10\%$ damping and stiffness uncertainty, the peak displacements at the highest floors were again increased compared to the uncontrolled case.

When considering the newly proposed controllers, the $RMPC_1$ had the best overall performance on dissipating the displacement and acceleration responses of the tower while having the highest power consumption. The $RMPC_2$ had the second best control performance while being the controller with the least power consumption in almost all cases. In contrast to the two RMPC schemes, the H_∞ could not keep the top floor displacements within the desired limit even though it had a good response dissipation performance. It is noted that, in the case were the parameter uncertainty was set to -10%, the small actuator capacity drove even the best of the two RMPC controllers to violate the tolerance requirement set for keeping the top floor dynamic displacements within ± 200 mm. Yet, the relative performance over the H_∞ is probably sufficient motivation for exploring robust algorithms that might perform even better.

It is concluded that the RMPC scheme is a very effective and powerful control method for civil engineering real mega-building applications. Future work will expand to consider (i) the semi-active capabilities of the hybrid system, which will be integrated within the control scheme in order to reduce the actuator energy requirements for dissipating the energy from the structure as shown in Figure 5, while allowing for control algorithm coupling between active and semi-active operating modes; (ii) an energy harvesting system, which will be designed in order to take advantage of the dissipative part of the energy, and decrease the energy requirements of the active control system and; (iii) artificial intelligence inspired controllers, which will be developed in order to account for non-linearities beyond uncertainty, and will be compared to conventional controllers in order to asses their performance.

ACKNOWLEDGEMENTS

The authors would like to thank GERB and Dr Christian Meinhardt for providing the hybrid TMD specifications, the initially-detailed finite-element model of the tower, and the wind loading design profiles. Additionally, the authors would like to thank the University of Leeds for providing the scholarship to the first author for conducting his doctoral studies.

CONFLICT OF INTEREST

The authors declare no potential conflict of interests.

DATA AVAILABILITY STATEMENT

The data that support the findings of this study are available from the corresponding author upon reasonable request.

ORCID

Nikolaos Nikitas https://orcid.org/0000-0002-6243-052X
Petros Aristidou https://orcid.org/0000-0003-4429-0225

REFERENCES

[1] J. N. Yang, S. Lin, F. Jabbari, *Struct. Control Health Monit.* **2004**, *11*(3), 223.
[2] Y. C. Ding, F. L. Weng, Z. A. Yu, *Shock Vib.* **2013**, *20*(2), 297.
[3] L. Wang, S. Nagarajaiah, W. Shi, Y. Zhou, *Struct. Des. Tall Spec. Build.* **2020**, *29*(15), 1.
[4] L. Wang, S. Nagarajaiah, W. Shi, Y. Zhou, *Eng. Struct.* **2021**, *244*(December 2020), 112743. https://doi.org/10.1016/j.engstruct.2021.112743
[5] L. Wang, W. Shi, Q. Zhang, Y. Zhou, *Eng. Struct.* **2020**, *209*(December 2019), 110010. https://doi.org/10.1016/j.engstruct.2019.110010
[6] C. W. Lim, Y. J. Park, S. J. Moon, *J. Sound Vib.* **2006**, *294*(1–2), 1.
[7] A. Mohtat, A. Yousefi-Koma, E. Dehghan-Niri, *Int. J. Struct. Stab. Dyn.* **2010**, *10*(3), 501.
[8] L. Koutsoloukas, N. Nikitas, P. Aristidou, Passive, semi-active, active and hybrid mass dampers: a literature review, Submitted, **2022**.
[9] A. Forrai, S. Hashimoto, H. Funato, K. Kamiyama, *Earthq. Eng. Struct. Dyn.* **2003**, *32*(11), 1655.
[10] I. Venanzi, *Struct. Multidiscip. Optim.* **2015**, *51*(1), 239.
[11] L. Wang, W. Shi, Y. Zhou, Q. Zhang, *Smart Struct. Syst.* **2020**, *25*(1), 65.
[12] D. Demetriou, N. Nikitas, K. D. Tsavdaridis, *The Struct. Des. Tall Spec. Build.* **2016**, *25*, 340.
[13] L. Wang, W. Shi, X. Li, Q. Zhang, Y. Zhou, *Struct. Control Health Monit.* **2019**, *26*(7), 1.
[14] A. J. Hillis, *Proc. Inst. Mech. Eng. Part I: J. Syst. Control Eng.* **2010**, *224*(1), 53.

[15] D. Demetriou, N. Nikitas, *Appl. Sci. (Switzerland)* **2016**, *6*(12), 397.
[16] H. Aggumus, R. Guclu, *Actuators* **2020**, *9*(3), 55.
[17] L. Huo, G. Song, H. Li, K. Grigoriadis, *Smart Mater. Struct.* **2008**, *17*(1), 15021.
[18] G. E. Stavroulakis, D. G. Marinova, E. Hadjigeorgiou, G. Foutsitzi, C. C. Baniotopoulos, *J. Wind Eng. Ind. Aerodyn.* **2006**, *94*(11), 895.
[19] L. Huo, C. Qu, H. Li, *The Struct. Des. Tall Spec. Build.* **2016**, *25*, 158.
[20] S. G. Wang, H. Y. Yeh, P. N. Roschke, *Proc. Am. Control Confer.* **2001**, *2*, 1109.
[21] S. Wang, P. N. Roschke, H. Y. Yeh, *J. Eng. Mech.* **2004**, *130*(March), 337.
[22] T. Tettamanti, T. Luspay, B. Kulcsar, T. Peni, I. Varga, *IEEE Trans. Intell. Transp. Syst.* **2014**, *15*(1), 385.
[23] M. Mirzaei, N. K. Poulsen, H. H. Niemann, Robust Model Predictive Control of a wind turbine, in 2012 American Control Conference (ACC) **2012**, 4393–4398.
[24] P. Langthaler, L. del Re, *IFAC Proc. Vol.* **2008**, *41*(2), 9485. https://doi.org/10.3182/20080706-5-KR-1001.01603
[25] K. Alexis, C. Papachristos, R. Siegwart, A. Tzes, *J. Intell. Robotic Syst.: Theory Appl.* **2016**, *81*(3-4), 443.
[26] M. Maasoumy, M. Razmara, M. Shahbakhti, A. S. Vincentelli, *Energy Build.* **2014**, *77*, 377. https://doi.org/10.1016/j.enbuild.2014.03.057
[27] H. Nagpal, A. Staino, B. Basu, Robust model predictive control of HVAC systems with uncertainty in building parameters using linear matrix inequalities, https://doi.org/10.1080/17512549.2019.1588165, **2019**.
[28] H. Peng, F. Li, Z. Kan, *J. Sound Vib.* **2020**, *471*, 115171. https://doi.org/10.1016/j.jsv.2020.115171
[29] H. Peng, F. Li, S. Zhang, B. Chen, *Comput. Struct.* **2017**, *187*, 35. https://doi.org/10.1016/j.compstruc.2017.03.014
[30] H. Peng, Y. Chen, E. Li, S. Zhang, B. Chen, *JVC/J. Vib. Control* **2018**, *24*(12), 2605.
[31] L. Koutsoloukas, N. Nikitas, P. Aristidou, C. Meinhardt, *Proc. Int. Confer. Struct. Dyn., EURODYN* **2020**, *1*, 1422.
[32] Y. Chen, S. Zhang, H. Peng, B. Chen, H. Zhang, *JVC/J. Vib. Control* **2017**, *23*(13), 2190.
[33] G. Mei, A. Kareem, J. C. Kantor, Model predictive control for wind Eexcited buildings: a benchmark problem, 14th Engineering Mechanics Conference, **2000**.
[34] F. Lopez-Almansa, R. Andrade, J. Rodellar, A. M. Reinhorn, *J. Eng. Mech.* **1995**, *120*(8), 1743.
[35] F. Lopez-Almansa, R. Andrade, J. Rodellar, A. M. Reinhorn, *J. Eng. Mech.* **1994**, *120*(8), 1761.
[36] G. Mei, A. Kareem, J. C. Kantor, *J. Eng. Mech.* **2002**, *128*(5), 574.
[37] G. Mei, A. Kareem, J. C. Kantor, *Earthq. Eng. Struct. Dyn.* **2001**, *30*(7), 995.
[38] G. Mei, A. Kareem, J. C. Kantor, *J. Eng. Mech.* **2004**, *103*, 459.
[39] W. M. Elhaddad, E. A. Johnson, *in Topics in Dynamics of Civil Structures*, vol. 4 **2013**, 27–36.
[40] Y. Wang, J. P. Lynch, K. H. Law, *Earthq. Eng. Struct. Dyn.* **2009**, *38*, 377.
[41] A. Acampora, J. H. G. Macdonald, C. T. Georgakis, N. Nikitas, *J. Wind Eng. Ind. Aerodyn.* **2014**, *124*, 90. https://doi.org/10.1016/j.jweia.2013.10.009
[42] G. Chase, A. Smith, T. Suzuki, *J. Eng. Mech.* **1996**, *122*(10), 984.
[43] A. Lago, D. Trabucco, A. Wood, Damping technologies for tall buildings, **2019**.
[44] A. Yonezawa, I. Kajiwara, H. Yonezawa, Model-free vibration control based on a virtual controlled object considering actuator uncertainty, JVC/-Journal of Vibration and Control, June, **2020**.
[45] A. Yonezawa, I. Kajiwara, H. Yonezawa, *IEEE Access* **2020**, *9*, 4351.
[46] T. R. Alt, F. Jabbari, J. N. Yang, *Earthq. Eng. Struct. Dyn.* **2000**, *29*(2), 241.
[47] S. G. Wang, *J. Eng. Mech.* **2004**, *130*(4), 511.
[48] Y. Ohtori, R. E. Christenson, B. F. Spencer, S. J. Dyke, *J. Eng. Mech.* **2004**, *130*(4), 366.
[49] J. N. Yang, A. K. Agrawal, B. Samali, J.-C. Wu, *J. Eng. Mech.* **2004**, *130*, 437.
[50] S. J. Dyke, J. M. Caicedo, G. Turan, L. A. Bergman, S. Hague, *J. Struct. Eng.* **2003**, *129*(7), 857.
[51] C. W. Lim, *Mechatronics* **2008**, *18*(8), 391.
[52] S. Narasimhan, *Struct. Control Health Monit.* **2009**, *16*, 599. https://doi.org/10.1002/stc.456
[53] A. Agrawal, P. Tan, S. Nagarajaiah, J. Zhang, *Struct. Control Health Monit.*, *16*, 509. https://doi.org/10.1002/stc.456
[54] S. N. Vassilyev, A. Y. Kelina, Y. I. Kudinov, F. F. Pashchenko, *Procedia Comput. Sci.* **2017**, *103*(October 2016), 623. https://doi.org/10.1016/j.procs.2017.01.088
[55] H. Du, N. Zhang, B. Samali, F. Naghdy, *Eng. Struct.* **2012**, *36*, 39. https://doi.org/10.1016/j.engstruct.2011.11.024
[56] M. A. Aly, *The Struct. Des. Tall Spec. Build.* **2014**, *23*, 664.
[57] N. Giron, M. Kohiyama, *Struct. Control Health Monit.* **2014**, *21*, 907. https://doi.org/10.1002/stc.456
[58] S. Skogestad, I. Postlethwaite, *Multivariable Feedback Control Analysis and Design*, 2nd ed., John Wiley and Sons Ltd, Sussex **2005**.
[59] D. Gill, S. Elias, A. Steinbrecher, C. Schröder, V. Matsagar, *Bull. Earthq. Eng.* **2017**, *15*(12), 5579.
[60] B. F. Spencer Jr., R. E. Christenson, S. J. Dyke, Next generation benchmark control problem for seismically excited buildings, in Second World Conference on Structural Control **1998**, 1135–1360. http://nees.org/resources/2405/download/Report_bldg_full2.pdf
[61] J. C. Doyle, Structured uncertainty in control system design., in Proceedings of the IEEE Conference on Decision and Control **1985**, 260–265.
[62] H. Adeli, H. Kim, *J. Struct. Eng.* **2004**, *130*(1), 128.
[63] B. F. Spencer, S. J. Dyke, H. S. Deoskar, *Earthq. Eng. Struct. Dyn.* **1998**, *27*(11), 1127.
[64] H. Kim, H. Adeli, *J. Struct.l Eng.* **2004**, *130*(1), 120.
[65] Y. Zhang, X. Zhao, X. Wei, *Wind Energy* **2020**, *October 2019*, 1.
[66] G. Takács, B. Rohalkiv, Model predictive vibration control, **2012**.
[67] S. K. Yalla, A. Kareem, J. C. Kantor, *Eng. Struct.* **2001**, *23*(11), 1469.
[68] F. Ricciardelli, A. D. Pizzimenti, M. Mattei, *Eng. Struct.* **2003**, *25*(9), 1199.
[69] S. Jeon, M. Tomizuka, *Control Eng. Practice* **2007**, *15*(3 SPEC. ISS.), 325.
[70] C. C. Lin, L. Y. Lu, G. L. Lin, T. W. Yang, *Eng. Struct.* **2010**, *32*(10), 3404. https://doi.org/10.1016/j.engstruct.2010.07.014
[71] T. T. Soong, *Active Structural Control: Theory and Practice*, John Wiley and Sons, Inc, New York **1990**.
[72] J. Lofberg, Approximations of closed-loop minimax MPC, in 42nd IEEE International Conference on Decision and Control **2003**, 1438–1442.
[73] J. Löfberg, Minimax approaches to robust model predictive control, http://www.control.isy.liu.se/research/reports/Ph.D.Thesis/PhD812.pdf, **2003**.

[74] J. Löfberg, YALMIP: a toolbox for modeling and optimization in MATLAB, in Proceedings of the IEEE International Symposium on Computer-Aided Control System Design **2004**, 284–289.
[75] L. Gurobi Optimization, Gurobi optimizer reference manual, **2021**.
[76] B. Palazzo, L. Petti, *J. Struct. Control* **1999**, *6*(2), 205.
[77] J. C. Wu, H. H. Chih, C. H. Chen, *J. Sound Vib.* **2006**, *294*(1–2), 314.
[78] C. Meinhardt, N. Nikitas, D. Demetriou, *Procedia Eng.* **2017**, *199*, 1719. https://doi.org/10.1016/j.proeng.2017.09.384
[79] H. Cao, A. M. Reinhorn, T. T. Soong, *Eng. Struct.* **1998**, *20*(3), 134.
[80] X. Lu, P. Li, X. Guo, W. Shi, J. Liu, *The Struct. Des. Tall Spec. Build.* **2014**, *23*, 105.
[81] I. Nagashima, R. Maseki, Y. Asami, J. Hirai, H. Abiru, *Earthq. Eng. Struct. Dyn.* **2001**, *30*(11), 1615.
[82] J. P. Den Hartog, *Mechanical Vibrations*, 4th ed., McGraw-Hill, New York, NY, USA **1956**.
[83] ANCO, Users guide: GERB TMD tower control system, ANCO ENGINEERS **2017**.
[84] N. Nikitas, J. H. G. Macdonald, J. B. Jakobsen, *Wind Struct.* **2011**, *14*(3), 221.
[85] J. Löfberg, *Optim. Methods Softw.* **2012**, *27*(1), 115.
[86] T. T. Soong, B. F. Spencer, *Bull. New Zealand Soc. Earthq. Eng.* **2002**, *33*(3), 387.
[87] R. Rana, T. T. Soong, *Eng. Struct.* **1998**, *20*(3), 193.
[88] L. Wang, W. Shi, Y. Zhou, *Struct. Des. Tall Spec. Build.* **2019**, *28*(1), e1561.
[89] K. Zhao, X. Lu, W. Zheng, C. Huang, Direct relaxation of hard-constraint in Model Predictive Control, in Proceedings - 2012 9th International Conference on Fuzzy Systems and Knowledge Discovery, FSKD 2012 **2012**, 2366–2370.
[90] M. N. Zeilinger, C. N. Jones, M. Morari, Robust stability properties of soft constrained MPC, in Proceedings of the IEEE Conference on Decision and Control **2010**, 5276–5282.
[91] M. Schwenzer, M. Ay, T. Bergs, D. Abel, *The Int. J. Adv. Manuf. Technol.* **2021**, *117*(5-6), 1327.

AUTHOR BIOGRAPHIES

Lefteris Koutsoloukas studied Civil & Strucutral Engineering in the University of Leeds and graduated with a 1st class honors. In 2019, he has been awarded a prestigious Leeds Doctoral Scholarship to pursue doctoral studies. Currently, he is a 2nd year PhD student working with Dr Nikolaos Nikitas and Dr Petros Aristidou. His research work lies within the area of structural dynamics where he focuses in the Active/Hybrid Control of civil engineering structures.

Nikolaos Nikitas graduated Civil Engineering from the Aristotle University of Thessaloniki, Greece, and subsequently received a PhD on Structural Mechanics from the University of Edinburgh, UK, and a PhD on Aerodynamics of Bridges from the University of Bristol, UK. He is currently working as an Associate Professor in Structural Dynamics and Engineering in the University of Leeds, UK, with research interest spanning from Structural Health Monitoring to wind and earthquake engineering.

Petros Aristidou received a Diploma in Electrical and Computer Engineering from the National Technical University of Athens, Greece, in 2010, and a PhD in Engineering Sciences from the University of Liège, Belgium, in 2015. He is currently a Lecturer at the Cyprus University of Technology. His research interests include sustainable energy, control, and simulation.

How to cite this article: L. Koutsoloukas, N. Nikitas, P. Aristidou, *Struct Design Tall Spec Build* **2022**, *31*(12), e1941. https://doi.org/10.1002/tal.1941